Articles

Interactions of *Acanthamoeba* Profilin with Actin and Nucleotides Bound to Actin†

Valda K. Vinson,‡,§,|| Enrique M. De La Cruz,‡,§,⊥,# Henry N. Higgs,⊥ and Thomas D. Pollard*,§,⊥

Department of Cell Biology and Anatomy, Johns Hopkins University School of Medicine 725 North Wolfe Street, Baltimore, Maryland 21205, and The Salk Institute, 10010 N. Torrey Pines Rd., La Jolla, California 92037

Received January 12, 1998; Revised Manuscript Received May 11, 1998

ABSTRACT: Three methods, fluorescence anisotropy of rhodamine-labeled profilin, intrinsic fluorescence and nucleotide exchange, give the same affinity, $K_d = 0.1$ μM, for *Acanthamoeba* profilins binding amoeba actin monomers with bound Mg-ATP. Replacement of serine 38 with cysteine created a unique site where labeling with rhodamine did not alter the affinity of profilin for actin. The affinity for rabbit skeletal muscle actin is about 4-fold lower. The affinity for both actins is 5−8-fold lower with ADP bound to actin rather than ATP. Pyrenyliodoacetamide labeling of cysteine 374 of muscle actin reduces the affinity for profilin 10-fold. The affinity of profilin for nucleotide-free actin is ∼3-fold higher than for Mg-ATP-actin and ∼24-fold higher than for Mg-ADP-actin. As a result, profilin binding reduces the affinity of actin 3-fold for Mg-ATP and 24-fold for Mg-ADP. Mg-ATP dissociates 8 times faster from actin−profilin than from actin and binds actin−profilin 3 times faster than actin. Mg-ADP dissociates 14 times faster from actin−profilin than from actin and binds actin−profilin half as fast as actin. Thus, profilin promotes the exchange of ADP for ATP. These properties allow profilin to bind a high proportion of unpolymerized ATP-actin in the cell, suppressing spontaneous nucleation but allowing free barbed ends to elongate at more than 500 subunits/second.

Rearrangement of the actin cytoskeleton during movements of eukaryotic cells depends, in part, on regulated polymerization and depolymerization of actin filaments. A large fraction of the total actin is unpolymerized (*1*−*3*), presumably bound to sequestering proteins. The concentration of unassembled actin is well above the concentrations (critical concentrations) required to elongate actin filaments, 0.1 μM at the fast-growing barbed end and 0.7 μM at the slow-growing pointed end for Mg-ATP-actin (*4*).

Accounting for this unassembled pool of actin has been a question for two decades. Several proteins have potential to sequester actin monomers. Profilin, a 13−15 kDa protein found in all eukaryotes examined (reviewed in ref *5*), binds actin monomers and catalyzes the exchange of nucleotide bound to actin (*6*−*8*). Profilin interferes with nucleation of new filaments and elongation at the pointed end of actin filaments, but its role as a sequestering protein is complicated by the ability of the actin−profilin complex to elongate barbed ends (*9*−*12*). Amoeba actobindin binds two actin monomers with micromolar affinity (*13*). Vertebrate thymosins bind actin monomers and inhibit polymerization (reviewed in ref *14*) but are not known to exist in lower eukaryotes. Members of the widespread ADF/cofilin family of actin-binding proteins (reviewed in ref *15*), including amoeba actophorin, bind both actin monomers and filaments. They depolymerize filaments, either by severing (*16*) or promoting dissociation of subunits from pointed ends (*17*), but do not inhibit elongation (*17*; L. Blanchoin and T. D. Pollard, submitted for publication).

To prevent the spontaneous polymerization of a large cellular pool of actin monomers, sequestering proteins must bind actin monomers in complexes that do not assemble. Thymosin and actobindin fulfill these criteria, but profilin requires the help of barbed end capping proteins. Further, the concentration of sequestering proteins must exceed that of the pool of unassembled actin and their affinity for actin must be sufficient to reduce the free actin concentration enough to suppress nucleation. Rarely, are the quantitative data available to know if the identified monomer-binding proteins can account for the unassembled pool of actin. In some cases, the protein concentrations in vivo are not known. In other cases, the equilibrium constants are not known or do not appear strong enough to account for the pool of unassembled actin. Our attention here is on profilin, the most abundant actin monomer binding protein in many cells, including *Acanthamoeba*.

† This work was supported by NIH Research Grant GM26338 to T. D. P., NIH Research Grant GM35171 to Eaton Lattman and TDP and an NSF Predoctoral Fellowship Award to E. M. D. L. C.

* To whom correspondence should be addressed. Phone: (619) 453-2340. Fax: (619) 452-3683. E-mail: pollard@salk.edu.

‡ V.K.V. and E.M.D.L.C. contributed equally to this work.

§ Johns Hopkins University School of Medicine.

|| Department of Biochemistry University of the Western Cape Bellville, 7535, South Africa.

⊥ The Salk Institute.

Department of Physiology, Pennsylvania Muscle Institute University of Pennsylvania School of Medicine, 3700 Hamilton Walk, Philadelphia, PA 19104.

S0006-2960(98)00093-2 CCC: $15.00
Published on Web 07/17/1998

The affinity of profilin for actin has been in question for years. The equilibrium constants vary with the type of profilin, the type of actin, the divalent cation and nucleotide bound to the actin, the ionic strength and modification of actin by pyrenyl labeling of Cys 374, or loss of the C-terminal phenylalanine residue. On top of these biological variables, the design of the assays and assumptions used to analyze the data also affect the interpretation. Assays fall into two classes: some measure interactions directly; others depend on an effect of profilin on actin function. An advantage of direct assays such as intrinsic fluorescence (*18*) is that no assumptions are required to interpret the consequences of interaction. Functional assays such as polymerization are essential to assess potential functions of the interaction, but are compromised by a major disadvantage, namely that interpretation requires assumptions regarding mechanism that may be difficult to verify. Ideally, one uses a direct assay to measure the thermodynamics and kinetics of interaction and then applies these values to interpret functional assays, rather than the reverse. In the case of profilin, the macromolecular partners include actin, Arp2/3 complex (*19*), proline-rich sequences in a number of proteins including VASP (*20*) and other proteins, and polyphosphoinositides (reviewed in ref *5*).

Since none of the available direct assays was ideal for the full range of ligands and experimental situations, including live cells, a new approach was useful. We sought an assay for profilin binding to actin that requires minimal assumptions for interpretation and is applicable for both kinetic and equilibrium measurements. We used site-directed mutagenesis to create sites for labeling *Acanthamoeba* profilin-II with the fluorescent dye rhodamine. As shown in this paper, fluorescence anisotropy of the rhodamine−profilin provides a direct assay for binding actin monomers. The absorbance of rhodamine−profilin-II at visible wavelengths provides a probe to assay equilibrium binding to actin and Arp2/3 complex by analytical ultracentrifugation (*21*). Fluorescence microscopy of rhodamine−profilin-II loaded into live cells allowed us to document the distribution and dynamics of profilin in vivo (D. A. Kaiser, V. K. Vinson, D. B. Murphy, and T. D. Pollard, submitted for publication).

Our second topic is the influence of profilin on the exchange of the nucleotide bound to actin. ADP-actin is released during the turnover of actin filaments, but most of the unpolymerized actin in cell extracts has bound ATP (*22*). Profilin enhances exchange of the nucleotide bound to actin and may be important to exchange ADP for ATP in the cell, where ADF/cofilin proteins inhibit exchange (*7*). To determine how profilin enhances nucleotide exchange, it is necessary to define a quantitative mechanism in thermodynamic and kinetic terms. Many of the rate and equilibrium constants are known for ATP- and ADP-actin (*12*, *18*, *23*). However, the affinity of profilin for nucleotide-free actin was inferred rather than measured directly due to lack of a preparation of pure nucleotide-free actin. Residual ATP-actin in earlier preparations (*24*, *25*) precluded firm conclusions about the capacity of nucleotide-free actin to bind profilin. A new preparation of actin 99% free of bound nucleotide allowed us to test its interaction with profilin and complete the thermodynamic and kinetic analysis of how profilin enhances nucleotide exchange.

EXPERIMENTAL PROCEDURES

Reagents. Salts, buffers, chemicals, fluorescent grade imidazole, grade I adenosine 5′-triphosphate (ATP), and grade VII potato apyrase were from Sigma Chemical Co. (St. Louis, MO). Sucrose (Ultrapure) came from GIBCO BRL (Gaithersburg, MD). Pyrenyliodoacetamide was from Molecular Probes (Eugene, OR).

Preparation of Mutant Profilin for Labeling. We used four primer polymerase chain reaction (PCR) mutagenesis (*26*) to convert residues S38, N47, N58, and A63 of *Acanthamoeba* profilin-II to cysteine. Since amoeba profilin-II has no cysteine, these new cysteines became specific and exclusive sites for attachment of a fluorescent probe. The coding region of each mutant was sequenced, using Sequenase 2.0 (U. S. Biochemicals). The mutant profilins in the pT5 expression vector were transformed into *Escherichia coli* strain BL-21(DE3) lysogenic for T7 polymerase. Expression and purification of mutant profilins was identical to that of wild-type profilin (*27*), except that 1 mM dithiothreitol (DTT) was included in all buffers to prevent oxidation. After elution from the poly-L-proline affinity column, profilins were refolded and stored in 20 mM Tris, pH 7.0, 20 mM KCl, and 1 mM DTT.

Fluorescent Labeling of Profilin-II. Approximately 75 μM recombinant profilin in reducing buffer was dialyzed for 2 h into labeling buffer (30 mM Tris, pH 8.0, 30 mM KCl, and 1 mM EDTA) and then reacted overnight at room temperature with an 8-fold molar excess of tetramethylrhodamine maleimide (mixed isomers, Catalog no. T489, Molecular Probes, Eugene, OR) from a 20 mM stock in DMSO. Addition of 10 mM DTT terminated the reaction. After clarification by ultracentrifugation, free dye was removed by gel filtration on Sephadex G25 equilibrated with 50 mM Tris, pH 7.5, 100 mM glycine, and 100 mM NaCl and affinity chromatography on poly-L-proline, eluting labeled profilin with 8 M urea in G25 buffer after a wash with 3 M urea in the same buffer. Labeled protein was refolded by dialysis against 20 mM Tris, pH 7.0, 20 mM KCl, and 1 mM DTT.

The concentration of rhodamine-labeled profilin was determined by densitometry of a Coomassie blue stained polyacrylamide gel after electrophoresis in SDS using unlabeled profilin standards and by the absorbance at 280 nm, corrected for the absorbance of rhodamine. The concentration of tetramethylrhodamine was estimated by absorbance at 541 nm using the molar extinction coefficients 90 000 M^{-1} cm^{-1} for rhodamine at 541 nm (Molecular Probes catalog) and 14 000 M^{-1} cm^{-1} for profilin at 280 nm (*28*). The absorbance of rhodamine at 280 nm was 30% of that at 541 nm. Therefore, we used the equation $(A_{280} - 0.3A_{541})/14000$ M^{-1} cm^{-1} to calculate the concentration of profilin. The concentration of free sulfhydryls was determined by absorbance after reaction with 5,5′-dithiobis(2-nitro)benzoic acid (DTNB, Sigma Chemical) (*29*).

Other Proteins. Actin was purified from *Acanthamoeba castellanii* (*30*) or rabbit skeletal muscle (*31*). Monomers were purified by gel filtration on Sephacryl S-300 in G-buffer (2 mM Tris, pH 7.5, 0.2 mM ATP, 0.1 mM $CaCl_2$, and 0.5 mM DTT) and used within 2 weeks. For some experiments, actin was labeled (*30*) with pyrenyliodoacetamide (Molecular Probes, OR). Extent of labeling was measured by absorbance

using extinction coefficients of 22 000 M^{-1} cm^{-1} at 344 nm for bound pyrene and 26 600 M^{-1} cm^{-1} at 290 nm (*32*) for actin after correction for pyrene (*33*). Mg-ATP actin was prepared by incubating Ca-ATP actin with 200 μM EGTA and 80 μM $MgCl_2$ for 5 min on ice. Mg-ADP-actin was prepared by treatment of Mg-ATP-actin with hexokinase and glucose (*30*). Nucleotide-free actin was prepared by mixing 250 μL of Ca-ATP G-actin treated with Dowex to remove free nucleotides and 850 μL of ice cold S-buffer (1 g sucrose plus 750 μL of 20 mM Tris, pH 8.0) containing 0.5 mM DTT and 500 μM EGTA (to decrease free [Ca^{2+}] and dissociate the bound ATP), equilibrating on ice for 5 min., then treating with 20 units/mL apyrase for 60 min on ice. This procedure removes >99% of ATP and ADP from the actin, which is still competent to polymerize in 50% sucrose with a critical concentration less than ATP-actin (E. De La Cruz and T. D. Pollard, submitted for publication). The final sucrose concentration is calculated to be 51% (w/v). In control samples, the 5 min preincubation with EGTA was omitted, 20 mM Tris buffer, pH 8.0, was substituted for apyrase, ATP and EGTA were added to 200 μM and $MgCl_2$ to 50−80 μM. This yields a solution of Mg-ATP-actin in 51% sucrose. Profilin-I and -II were purified from *A. castellanii* (*10*). Dr. Vivianne Nachmias of the University of Pennsylvania kindly provided thymosin-β4.

Fluorescence Spectroscopy. Fluorescence data were collected on a PTI Alphascan spectrofluorimeter (Photon Technology International, Santa Clara, CA). Fluorescence anisotropy, r, is defined as

$$r = (I_V - GI_H)/(I_V + 2GI_H) \quad (1)$$

where I_V and I_H are the parallel and perpendicular components of the polarized fluorescence light and G is a correction factor to account for instrumental differences in detecting the emitted components. I_V and I_H were recorded simultaneously using a T-format with sheet polarizers. Rhodamine-labeled profilin was excited with polarized light at 549 nm, and horizontal and vertical components of the emitted light were detected at 573 nm. Measurements were made for 40 s at 5 points/s, and the average anisotropy was calculated using the data processing software Felix (Photon Technology International, Santa Clara, CA). The G factor was determined for the protein solution excited with horizontally polarized light.

Bound actin does not change the fluorescence of rhodamine−profilin-II, so the observed anisotropy is a linear function of the fraction of profilin with bound to actin

$$r = r_f + (r_b - r_f)\,([P_b]/[P]) \quad (2)$$

where r_f is the anisotropy of free profilin, r_b is the anisotropy of the complex, P_b is the bound profilin concentration, and P is the total concentration of profilin.

At any total concentration of profilin [P], r depends on the total actin [A] and the dissociation equilibrium constant for the complex (K_d) according to eq 3.

$$r = r_f + (r_b - r_f)\left(\frac{(K_d + [P] + [A]) - \sqrt{(K_d + [P] + [A])^2 - (4[P][A])}}{2[P]}\right) \quad (3)$$

Fitting this equation to titration data yields the amplitudes ($r_b - r_f$), the anisotropy value of the free profilin (r_f) and the affinity.

In cases where $[P] < K_d$, essentially all of the added actin is free ($[A] = [A_f]$) and eq 3 simplifies to the hyperbolic function

$$r = r_f + (r_b - r_f)[A_f]/(K_d + [A_f]) \quad (4)$$

Competition Experiments. If a second nonfluorescent ligand competes with labeled profilin for binding actin, then the concentration of free actin is

$$[A_f] = [A_o] - [L][A_f]/K_2 \quad (5)$$

which can be rearranged to give

$$[A_f] = K_2[A_o]/([L] + K_2) \quad (6)$$

where [L] is the concentration of the competing ligand, K_2 is the dissociation equilibrium constant of its complex with actin, and $[A_o]$ is the free actin concentration at $[L] = 0$. Substituting eq 6 into eq 4 gives

$$r = r_f + (r_b - r_f)/[(K_d([L] + K_2)/K_2[A_o]) + 1] \quad (7)$$

Provided the competing ligand is in excess, the concentration of free ligand is approximately equal to the total concentration. If K_d is known, $[A_o]$ can be calculated and a plot of observed anisotropy versus concentration of competing ligand, can be fitted to give K_2.

Intrinsic Fluorescence Measurements. Tryptophan intrinsic fluorescence was measured on a MD-5020 spectrofluorimeter (Photon Technology International), with excitation at 295 nm and emission at 327.5 nm (*18*). Samples contained 2 mM Tris-Cl, pH 8.0, 0.2 mM ATP or ADP, 0.1 mM $MgCl_2$ or $CaCl_2$, and 0.5 mM DTT. Profilin was titrated into a fixed concentration of actin (0.1 μM for *Acanthamoeba* actin and 0.25 μM rabbit skeletal muscle actin) from a concentrated stock containing the same actin concentration. The starting volume in the cuvette was 2.25 mL, and readings were taken after 5, 10, or 20 μL aliquots of the profilin/actin solution were added, up to a volume of 2.5 mL. Conversion of raw data was carried out as follows:

$$\Delta F = F_p - (F_{pa} - F_a)$$

where ΔF is the difference in intrinsic fluorescence between profilin alone (F_p) and profilin with saturating actin (F_{pa}). F_a is the fluorescence of actin alone. ΔF is proportional to the concentration of profilin−actin complex (*18*). A plot of ΔF vs [profilin] is fit to give a K_d for the interaction.

Kinetics. The time course for the dissociation of rhodamine−profilin from actin was determined from the reduction in anisotropy after mixing with >10-fold excess of unlabeled profilin. Rhodamine−profilin bound to actin was mixed with unlabeled *Acanthamoeba* profilin II using a hand-driven model SFA-12 Rapid Kinetics Stopped-Flow

FIGURE 1: Stereo ribbon diagram of *Acanthamoeba* profilin-II based on the crystal structure of Fedorov et al. (*37*) drawn using Setor software. The side chains of residues S38, N47, N58, and A63 are shown as space filling. These individual residues were replaced with cysteine to allow specific labeling with rhodamine-maleimide. van der Waals surface contours of residues involved in actin binding (*38*) and poly-L-proline binding (*39*) are shown as dots with the actin binding surface on the left and back at lower density than the poly-L-proline binding surface on the right.

Accessory (Hi-Tech Scientific Ltd., Salisbury, U.K.) with a dead time of about 50 ms. The time course of dissociation fit a single exponential.

Nucleotide Exchange in the Presence of Profilin. The dissociation rate constant of the nucleotide was determined from the time course of fluorescence change after mixing equal volumes of 2.8 μM Mg-ϵATP or Mg-ϵADP *Acanthamoeba* actin with native *Acanthamoeba* profilin-II in 2 mM $MgCl_2$, 600 μM ATP, and 2 mM Tris (pH 8.0) buffer. Measurements were made on a PTI Alphascan fluorimeter equipped with a Hi-Tech SFA-12 rapid mixer. Time courses were fitted to single-exponential functions. The profilin concentration dependence of the nucleotide dissociation rate was fitted to a form of eq 1.

RESULTS

Characterization of Labeled Proteins. We used *Acanthamoeba* profilin-II for these experiments, since it lacks cysteine residues (*33*) and binds well to actin (*10*), poly-L-proline (*35*), and polyphosphoinositides (*36*). We mutated four residues, S38, N47, N58, and A63, to cysteine (Figure 1) for reaction with rhodamine maleimide. We selected these residues based on the following criteria: (i) each residue is variable in profilins from across the phylogenetic tree, with a cysteine or serine present at three of the four positions in another profilin sequence in the database; (ii) each residue is at least partially exposed to solvent in the crystal structure (*37*); and (iii) none of the residues participates in the binding sites for actin (*38*) or poly-L-proline (*39*).

Reaction of mutant profilins with mixed isomers of rhodamine maleimide for 16 h at room temperature labels the single cysteine of 20−30% of each of the four mutant profilins, based on absorbance at 280 and 541 nm. The extinction coefficient of rhodamine bound to the protein is not known, so the stoichiometry is not determined precisely; however, reaction of the labeled protein with DTNB gave similar results. Reactions are much slower at 4 °C. The reaction of DTNB with unlabeled mutant profilins is also slow, taking 20 min to reach 80−90% completion at room temperature. These slow reactions indicate that none of the engineered sulfhydryls is well exposed to solvent. Prior to labeling, protein is dialyzed into labeling buffer containing EDTA (to chelate heavy metals) for 2 h at 4 °C to minimize oxidation, but oxidation probably competes with tetramethylrhodamine maleimide for the cysteines. Termination of the labeling reaction with 10 mM DTT should reduce any oxidized unlabeled protein. Twenty to thirty percent labeling is sufficient for the biochemical experiments reported here and for observing profilin in live cells by fluorescence microscopy. Unlabeled profilin does not interfere with quantitative measurements of actin binding to labeled profilin, since both profilins have the same affinity for actin (see below). The new 5′ and 6′ purified isomers of rhodamine maleimide now provided by Molecular Probes require modified labeling protocols that we are still perfecting.

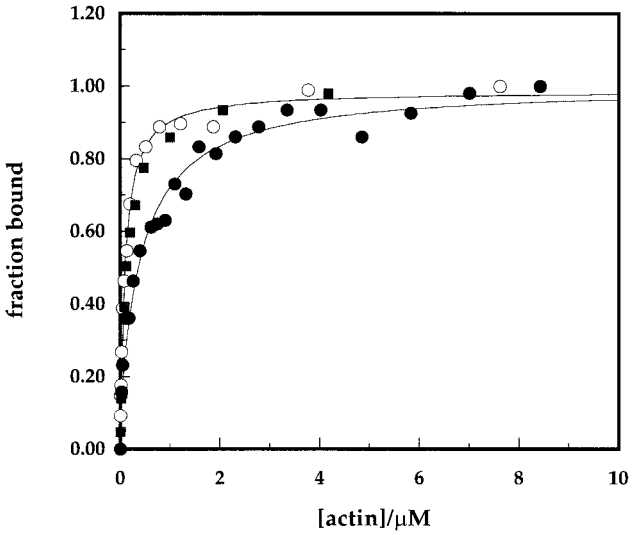

FIGURE 2: Fluorescence anisotropy assay for the binding of rhodamine-labeled S38C-profilin-II to *Acanthamoeba* Mg-ATP- and Mg-ADP-actin. Conditions: 2 mM Tris pH 8.0, 0.2 mM ATP or ADP, 1 mM DTT, 0.1 mM $MgCl_2$, 22 °C. Rhodamine-labeled S38C-profilin-II (75 nM) was titrated with solutions of ATP-actin (open circles) or ADP-actin (filled circles) containing 75 nM rhodamine-labeled S38C-profilin-II. A sample of Mg-ADP-actin was reconverted to Mg-ATP-actin by addition of 1 mM ATP and titrated into profilin to reconstitute higher affinity binding (filled squares). Data are fit with eq 3, yielding the equilibrium constants in Table 1.

Rhodamine-labeled profilin-II S38C and N58C bind actin with the same affinity as native profilin-II, as detailed below. These labeled profilins have a fluorescent anisotropy of 0.10, independent of dilution, as expected for a 13 kDa monomeric protein. Rhodamine-labeled S38C and N58C profilins are homogeneous monomers when analyzed by sedimentation equilibrium analytical ultracentrifugation and measuring either absorbance at 550 nm (for rhodamine) or at 280 nm (for protein) (*21*). Attempts to achieve higher levels of labeling of S38C resulted in rhodamine−profilin-II with higher r_f values, perhaps due to aggregation, so these preparations were not used. Labeling with rhodamine iodoacetamide gave less than 10% labeling with N58C profilin-II and precipitated S38C profilin-II. The r values of rhodamine-labeled A63C and N47C were slightly higher and changed little upon the addition of actin, so they were not used for quantitative analysis. All four rhodamine-labeled profilin-II mutants bind the poly-L-proline affinity column and elute under the same conditions as unlabeled, wild-type profilin-II.

Binding to Actin. Fluorescence anisotropy is a direct assay to measure binding of rhodamine−profilin-II to actin (Figure 2). The r value is 0.22 in the presence of saturating concentrations of monomeric actin, as expected for a globular

Table 1: Dissociation Equilibrium Constants (μM) for Profilin-Binding Actin Monomers[a]

	amoeba actin			muscle actin	
bound ligands	fluorescence anisotropy	intrinsic fluorescence	nucleotide exchange	fluorescence anisotropy	intrinsic fluorescence
Mg-ATP-actin	0.10 ± 0.01	0.10 ± 0.01	0.11	0.48 ± 0.06	1.01 ± 0.06
Mg-ATP in 50 mM KCl		0.20 ± 0.02			2.06 ± 0.18
Mg-ATP-actin in 50% sucrose	0.02				
nucleotide-free-actin in 50% sucrose	0.006				
nucleotide-free-actin in buffer	0.035 (calculated)				
Mg-ADP-actin	0.45 ± 0.04	0.41 ± 0.04	0.84	2.06 ± 0.54	1.06 ± 0.10
Ca-ATP-actin	0.17 ± 0.02	0.24 ± 0.05		0.55 ± 0.05	
Ca-ATP-pyrenyl actin				5.26 ± 0.46	

[a] All values for *Acanthamoeba* profilin-II, except intrinsic fluorescence measurements, which were made with a mixture profilin-I and profilin-II. Errors are deviations from theoretical binding isotherms.

complex of 57 kDa (*40*). Equation 3 fits well the dependence of the *r* value on the concentration of actin monomers and yields the equilibrium constant of the complex (Table 1).

The affinity of S38C-rhodamine−profilin-II for actin depends on the source of the actin, the bound nucleotide, and bound divalent cation (Table 1). In less extensive experiments with rhodamine-labeled N58C profilin-II, we obtained identical binding constants, suggesting that the locations of these two probes do not affect interaction with actin. Irrespective of the divalent cation and bound nucleotide, the affinity of *Acanthamoeba* profilin-II is about 4-fold higher for amoeba actin than rabbit skeletal muscle actin, as noted previously with polymerization assays (*41, 42*). For both actins, the affinity for profilin is about 5-fold higher with ATP-bound to the actin rather than ADP. To confirm that this difference in affinity is not due to denaturation of ADP-actin, we regenerated ATP-actin and found that the higher affinity was restored (Figure 2). The metal ion bound to actin has a small, but significant effect on profilin binding, with Mg^{2+} favoring actin binding slightly compared with Ca^{2+}. Labeling muscle actin cysteine 374 with pyrenyliodoacetamide reduces affinity for profilin 10-fold. Less quantitative assays originally suggested that profilin does not bind pyrenyl actin at all (*43*).

Competition Experiments. To determine if rhodamine labeling affects actin binding, we titrated unlabeled profilin into a constant concentration of actin and rhodamine-S38C−profilin (Figure 3A). We used eq 7 and the binding constant for rhodamine-S38C−profilin-II to calculate the affinity of the competing ligand for actin monomers. Dissociation equilibrium constants of unlabeled and labeled profilin are the same within experimental error. Similar competition experiments gave binding constants for *Acanthamoeba* profilin-I (Table 2) that differed by less than a factor of 2 from those of profilin-II.

Thymosin-β4 competes with labeled profilin for binding actin monomers (Figure 3B, Table 2), confirming that their binding sites on actin overlap, as suggested by chemical cross-linking experiments (*44, 45*). The 50-fold difference in the equilibrium constants for ATP- and ADP-actin agree with those measured from the effect of thymosin-β4 on the critical concentration for actin polymerization (*46*).

Intrinsic Fluorescence Measurements. To confirm the results obtained by fluorescence anisotropy, we measured profilin binding to actin using the intrinsic fluorescence assay of Perelroizen et al. (*18*) (Figure 4). The two assays gave the same values for native profilin binding Mg-ATP-, Ca-ATP-, and Mg-ADP-amoeba actin (Table 1). Furthermore, the affinities of rhodamine-labeled S38C profilin-II and native profilins for Mg-ATP-amoeba actin are similar. The affinity of amoeba profilin for Mg-ATP actin from both amoeba and muscle is about 2-fold-lower in 50 mM KCl than in low salt (Figure 4 and Table 1). This concentration of KCl quenches the fluorescence about 3% [less than reported by Perelroizen et al. (*18*)], but does not preclude measurement of the interaction of the two proteins.

Measurements on rabbit muscle actin by intrinsic fluorescence differ from those obtained by anisotropy in two ways. First, the apparent K_d values from intrinsic fluorescence are about 2-fold higher. Second, intrinsic fluorescence gives the same affinities for Mg-ATP- and Mg-ADP-muscle actin, as observed by Perelroizen et al. (*18*) for bovine spleen profilin.

Kinetics of Profilin Binding to Actin Monomers. We determined the rate constants for dissociation of rhodamine-S38C−profilin-II from Ca-ATP-, Mg-ATP-, and Mg-ADP-*Acanthamoeba* actin by stopped-flow fluorescence anisotropy (Figure 5, Table 3). Rate constants were obtained from the average of four measurements. Faster dissociation accounts for the slightly lower affinity of profilin for Ca-actin than Mg-actin. The difference in dissociation rate constants for ATP- and ADP-actin does not explain the 5-fold difference in affinity and suggests that profilin binds ADP-actin slower than ATP-actin.

Interaction of Nucleotide-Free Actin with Profilin. We used fluorescence anisotropy to compare the affinity of rhodamine-labeled *Acanthamoeba* profilin-II for *Acanthamoeba* actin with bound Mg-ATP or free of nucleotide in 50% sucrose. Sucrose prevents the denaturation of nucleotide-free actin monomers. Mg-ATP actin binds profilin with a dissociation equilibrium constant of 19 nM (Figure 6), 5 times more strongly than without sucrose. In 50% sucrose, nucleotide-free actin binds profilin 3 times stronger than Mg-ATP actin (K_d = 6 nM).

The complex of nucleotide-free actin with profilin is one of the intermediates in the process of actin nucleotide exchange enhanced by profilin, so to provide a consistent set of rate and equilibrium constants for the mechanism, we reexamined the effect of profilin on actin nucleotide exchange in the presence of a physiological concentration of Mg^{2+} (Figure 7). Profilin increases the rate of nucleotide exchange in a concentration-dependent manner. In 1 mM $MgCl_2$ buffer without sucrose, saturating profilin increases the rate of ϵATP dissociation 8-fold from 0.024 to 0.19 s^{-1} (Figure 7B).

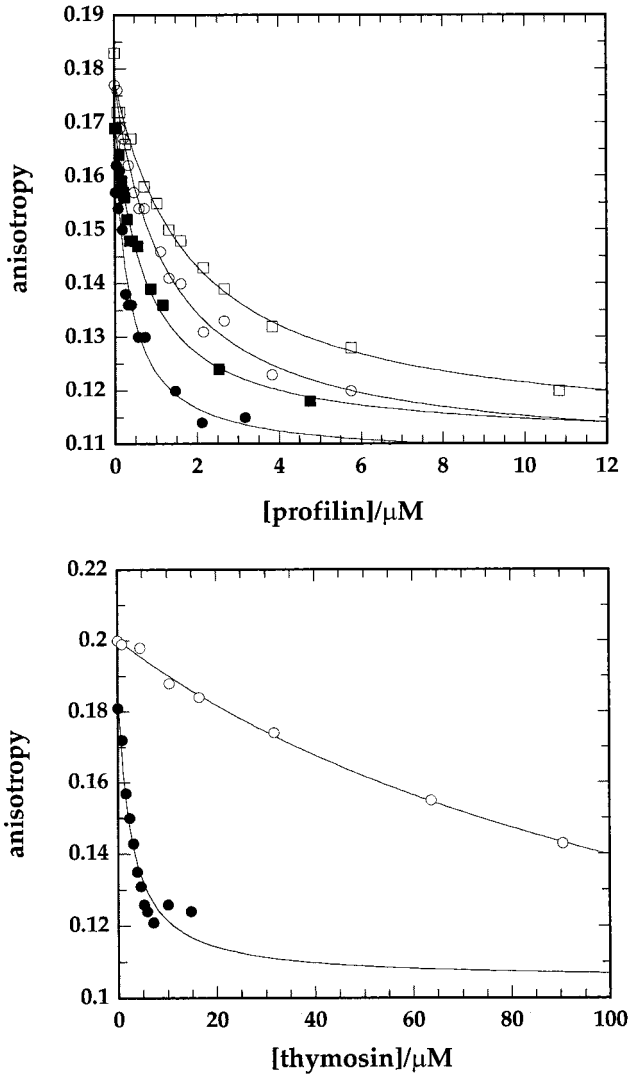

FIGURE 3: Fluorescence anisotropy assay for competition between rhodamine-labeled S38C-profilin-II and unlabeled profilin for binding to actin. Conditions: 2 mM Tris pH 8.0, 0.2 mM ATP or ADP, 1 mM DTT, 0.1 mM $MgCl_2$, 22 °C. (Upper panel) 75 nM rhodamine-labeled S38C-profilin-II with 0.2 μM *Acanthamoeba* ATP-G-actin (filled symbols) or 0.5 mM *Acanthamoeba* Mg-ADP-actin (open symbols) was titrated with unlabeled *Acanthamoeba* profilin-I (squares) or profilin-II (circles), containing the same concentrations of actin and labeled profilin. The curves were fitted to eq 7 to obtain the equilibrium constants listed in Table 2. (Lower panel) Rhodamine-labeled S38C-profilin-II (75 nM) with 0.5 μM rabbit skeletal muscle Mg-ATP-actin (filled circles) or 3.0 μM rabbit skeletal muscle Mg-ADP-actin (open circles) were titrated with thymosin-β4. The concentrations of actin and labeled profilin were maintained constant throughout the titration. Data are fit with eq 7, yielding the equilibrium constants in Table 2.

Perelroizen et al. (*23*) reported a much larger enhancement of the exchange rate from 0.054 to 2.1 s^{-1} with different profilin and actin in 1 mM Mg Cl_2 and 100 mM KCl. The affinity of profilin for Mg-ATP-actin determined from the exchange data is 110 nM, identical to the affinity measured by fluorescence anisotropy and intrinsic fluorescence. The results are similar when bound ATP is exchanged for ϵATP. Saturating profilin increases the rate of exchange of Mg-ϵADP 14 times (Figure 7B). The profilin concentration dependence gives a K_d of 840 nM similar to the value of 500 nM obtained by fluorescence anisotropy.

Table 2: Fluorescence Anisotropy Assay for Competition between Unlabeled Proteins and S38C-Rhodamine Profilin-II Binding Actin[a]

unlabeled protein	actin	K_d (μM)
amoeba profilin-II	amoeba Ca-ATP-actin	0.20 ± 0.05
amoeba profilin-I	amoeba Ca-ATP-actin	0.41 ± 0.04
amoeba profilin-II	amoeba Mg-ADP-actin	0.66 ± 0.08
amoeba profilin-I	amoeba Mg-ADP-actin	0.97 ± 0.14
thymosin-β4	muscle Mg-ATP-actin	1.17 ± 0.36
thymosin-β4	muscle Mg-ADP-actin	53.5 ± 13.7

[a] Errors are the deviation of the data from eq 7.

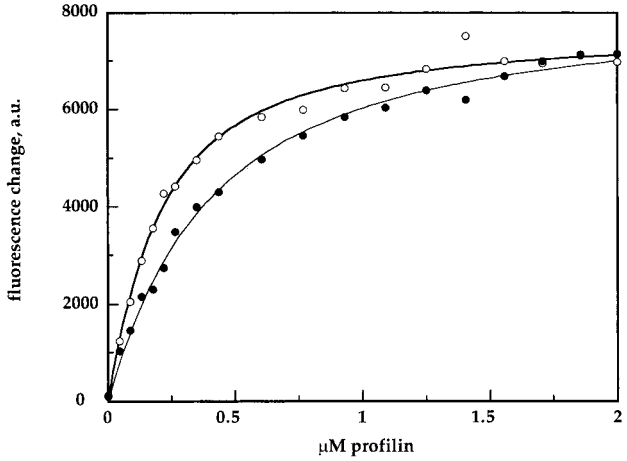

FIGURE 4: Instrinsic fluorescence assay for native amoeba profilin binding to actin monomers. Conditions: 2 mM Tris pH 8.0, 0.2 mM ATP, 0.1 mM $MgCl_2$, 0.5 mM DTT, ± 50 mM KCl, 0.1 μM *Acanthamoeba* actin, 22 °C. The sample was titrated by adding aliquots of concentrated stock of amoeba profilin containing the same actin concentration in the same buffer. The curves are least-squares fit to the data. No KCl (open circles) or 50 mM KCl (filled circles).

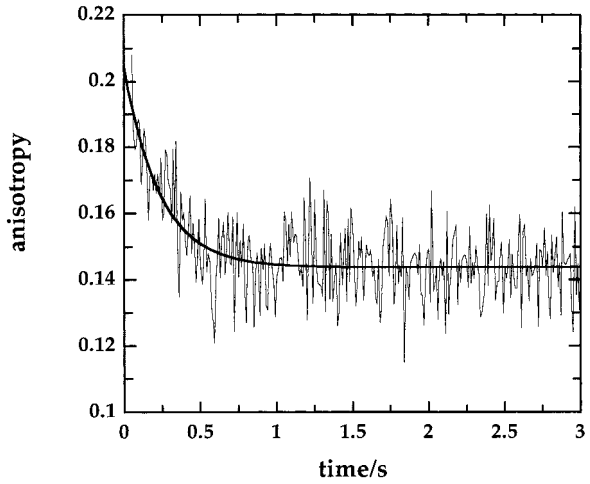

FIGURE 5: Time course of dissociation of the profilin-actin complex. Conditions: 2 mM Tris pH 8.0, 0.2 mM ATP or ADP, 1 mM DTT, 0.1 mM $MgCl_2$, 22 °C. Syringe 1 contained 0.8 μM rhodamine-labeled S38C-profilin-II and 0.8 μM *Acanthamoeba* Mg-ATP-actin. Syringe 2 contained 10 μM unlabeled *Acanthamoeba* profilin. Equal volumes of the two reactants were mixed to start the reaction. The displacement of labeled profilin by unlabeled profilin was accompanied by a decrease in anisotropy. The time course was fitted to a single exponential to give a rate constant of 4.3 ± 0.5 s^{-1} for dissociation of profilin from Mg-ATP actin.

DISCUSSION

Comparison of Actin-Binding Assays. Rhodamine-labeled profilins provide a direct fluorescence anisotropy assay to

Table 3: Kinetics of Profilin Binding to Actin Monomers by Stopped-Flow Fluorescence Anisotropy

actin	measured K_d (μM)	measured k_- (s^{-1})	calculated k_+ (μM^{-1} s^{-1})
amoeba Mg-ATP actin	0.10 ± 0.01	4.3 ± 0.5	35−53
amoeba Ca-ATP actin	0.17 ± 0.02	6.6 ± 0.8	34−57
amoeba Mg-ADP actin	0.45 ± 0.04	10.9 ± 2.5	17−33

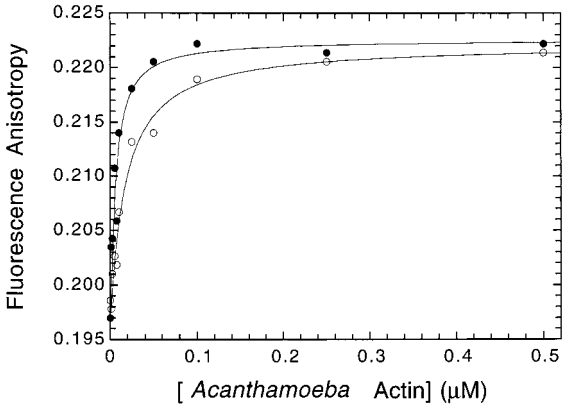

FIGURE 6: Profilin binds to ATP and nucleotide-free actin. Binding was determined from the fluorescence anisotropy of S38C labeled *Acanthamoeba* profilin-II. Conditions: 20 mM Tris (pH 8.0), 51% sucrose, 23.3 nM profilin, $\lambda_{ex} = 549$ nm, $\lambda_{em} = 573$ nm, 22 °C. The solid lines are the best fits to eq 1. The K_ds determined from the fits are 0.019 μM for Mg-ATP-actin (open circles) and 0.006 μM for nucleotide-free actin (filled circles)

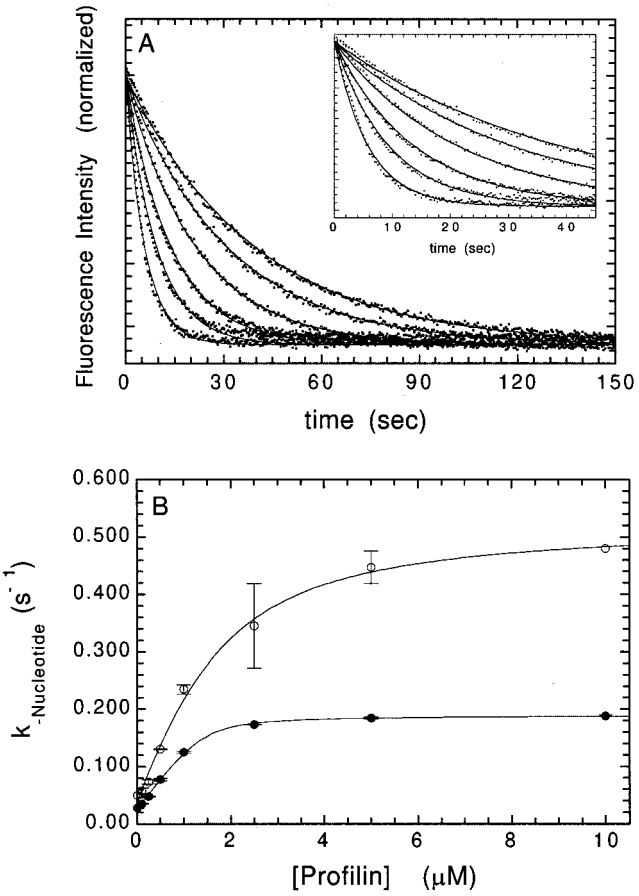

FIGURE 7: Profilin increases the rate of nucleotide dissociation from actin. (A) Time course of fluorescence change after mixing 1.4 μM *Acanthamoeba* Mg-ϵATP-actin with *Acanthamoeba* profilin-II and 300 μM ATP in 1 mM $MgCl_2$ buffer at 22 °C. Curves from left to right are 10, 1.0, 0.5, 0.25, 0.10, and 0 μM profilin. Amplitudes are equal for all traces. The inset shows the early times of the transients. Solid lines are the best fits to single exponentials. (B) Profilin concentration dependence of the nucleotide dissociation rate. (filled circles) Mg-ϵATP-actin, (open circles) Mg-ϵADP-actin. The K_ds determined from the fits to eq 1 are 0.11 μM for ATP and 0.84 μM for ADP-actin. Error bars represent the standard deviations of three to five replicate measurements.

evaluate binding to cytoplasmic and skeletal muscle actins. This assay has advantages over previous methods to study the interaction of profilin with actin. Placement of the rhodamine well away from the known ligand-binding sites avoids interference with these interactions. The absorbance of rhodamine allows measurement of profilin concentrations in mixtures with unlabeled proteins, which is convenient to study interactions by analytical ultracentrifugation (*21*). Rhodamine profilin can also be used to study the dynamics of profilin in live cells. Tarachandani and Wang (*47*) prepared a fluorescent derivative of rat profilin-I for microinjection studies, but did not use the fluorescence to study binding to actin.

Fluorescent dyes at the interface of actin and profilin, such as pyrene on actin cys 374, are sensitive to the interaction of the proteins (*48*). The signal from the pyrene yielded the correct equilibrium constant for profilin binding to pyrene-labeled Ca-ATP muscle actin (5 μM), but the pyrene reduces the affinity (*43, 49*), measured for the first time in this study to be 10-fold less. Earlier reports stated that pyrene-actin does not bind profilin.

Actin polymerization assays that were used in the initial studies of actin−profilin interaction (*41, 42, 49*) are complicated by reactions of profilin and profilin−actin with the barbed end of actin filaments (*9*−*12*). Polymerization assays employing only the pointed end of actin filaments (i.e., with the barbed end capped) give the correct equilibrium constant (*12, 50*). This strongly supports models of profilin action where the actin−profilin complex cannot elongate pointed ends (*9*−*12*). Filtration assays for profilin-binding actin monomers (*8*) should be free of these complications but gave high values for the dissociation equilibrium constant.

Profilin binding quenches the tryptophan fluorescence of actin by about 25%, providing an assay for both equilibrium and kinetics experiments (*18*). This assay with unlabeled proteins is more convenient than fluorescence anisotropy, but the signal-to-noise ratio is low and the method is not applicable to complex mixtures of proteins or to live cells. Intrinsic fluorescence also gives one result that is not confirmed by other reliable assays. By intrinsic fluorescence, amoeba profilin and bovine spleen profilin (*18*) bind muscle ATP- and ADP-actin with the same affinity. Fluorescence anisotropy (current report), polymerization assays (*12*), and nucleotide exchange (*23*; current report) all indicate that both profilins have a higher affinity for muscle ATP-actin than ADP-actin. We have no explanation for this anomaly.

Affinity of Profilin for Actin. Affinity of profilin for actin depends on the type of actin, the bound nucleotide, and divalent cation. Affinity is highest for cytoplasmic actin without nucleotide, followed by cytoplasmic Mg-ATP actin. In 1 mM Mg^{2+}, the affinity is only slightly lower in 50 mM KCl than no salt, so ionic conditions have little effect on binding. Affinity is lower for Mg-ADP actin even though polymerization assays (*49*) had suggested that the affinity of amoeba profilin for Mg-ADP-actin ($K_d = 1-2$ μM) is

Scheme 1

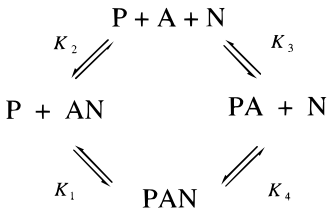

higher than for Mg-ATP actin (K_d = 5 μM). Our results with ADP-actin agree with the experiments of Perelroizen et al. (*23*) on bovine profilin. The affinity of amoeba profilin is also 4-fold lower for muscle actin, a reminder that actins differ among species and cell types, so that homogeneous systems are necessary to provide the rigorous quantitative data that are required to advance our understanding of actin-binding proteins and cellular dynamics.

Effect of Profilin on Nucleotide Exchange by Actin. During rapid filament turnover in motile cells, ADP-actin is released from filaments and slow dissociation of Mg-ADP from these actin subunits (half time 35−70 s depending on conditions; refs 51, 18, current report) is rate limiting prior to ATP binding and high-affinity association of ATP-actin with profilin or thymosin-β4. Profilin accelerates (*6*) and ADF/cofilin proteins inhibit (*7*) nucleotide exchange. At steady state, most of the unpolymerized actin has bound ATP, at least in cellular extracts (*22*).

Knowledge of the affinity of profilin for nucleotide-free actin provides the information required to explain thermodynamically how profilin enhances nucleotide exchange. Binding of nucleotide and divalent cations is coupled, especially in 1 mM $MgCl_2$ (*52*), so we consider them together here as a cation−nucleotide complex, N in Scheme 1. The new experiments were performed in 50% sucrose, because nucleotide-free actin denatures rapidly and irreversibly without stabilizers. To interpret these data, we assume that sucrose has the same effect on profilin binding to nucleotide-free actin and Mg-ATP actin. This assumption is supported by the following observations and by detailed balance. (i) Sucrose does not affect the affinity of actin for Mg-ϵATP (K_d = 4.4 nM in water and 5.1 nM in 50% sucrose), although both the association and dissociation rate constants are lower in sucrose (*25*). (ii) In both dilute buffers (Figure 4) and 50% sucrose (data not shown), Mg-ATP dissociates 7 times faster from the actin−profilin complex than from actin alone, so sucrose does not affect the affinity of actin for nucleotide or the mechanism of nucleotide exchange by profilin. Thus, to maintain detailed balance, the affinity of profilin for actin with and without bound nucleotide must be affected to the same extent by sucrose. Given that the affinity of profilin for nucleotide-free actin is 3 times higher than for Mg-ATP actin in high sucrose (Figure 3) and that the affinity of profilin for Mg-ATP actin is about 4 times higher in high sucrose than dilute buffer (Figure 4B), we calculate that the K_d for the complex of profilin and nucleotide-free actin in buffer without sucrose is about 35 nM (K_a = 0.029 nM^{-1}).

Therefore, in low sucrose buffer with 1 mM Mg^{2+}, the equilibrium constants for the Mg-ATP exchange cycle in Scheme 1 have the following values: going clockwise, K_1 = 110 nM; K_2 = 1.2 nM (*25*); and K_3 = 0.029 nM^{-1}. Since the product of equilibrium constants in a cyclic path equals 1, K_4 = 0.26 nM^{-1} (K_d = 3.8 nM). Thus, the binding of profilin to actin without bound nucleotide lowers the affinity of actin about 3-fold for Mg-ATP. For a Mg-ADP exchange cycle, the equilibrium constants have the following values: K_1 = 840 nM (from Figure 7), K_2 = 4.8 nM [since Mg-ADP binds about 4 times weaker than Mg-ATP (*52*)], K_3 = 0.029 nM^{-1} and, therefore, K_4 = 0.0086 nM^{-1} (K_d = 116 nM). Thus, the higher affinity of profilin for nucleotide-free actin lowers the affinity of actin 24-fold for Mg-ADP.

Our results agree in general with extensive studies of Perelroizen et al. (*18*, *23*). We agree that the affinity of profilin for Mg-ATP actin (amoeba in our case and muscle in theirs) is 0.1 μM. We find that the affinity for Mg-ADP actin is 5−8-fold lower, while they measured 30-fold lower in the nucleotide exchange assay and no difference by intrinsic fluorescence. They estimated that the affinity of Ca-ATP for actin−profilin complex is 100 times lower than for actin alone from nucleotide exchange experiments in very low salt and Ca^{2+}, while our values calculated from detailed balance are 3-fold lower for Mg-ATP and 24-fold lower for Mg-ADP. By detailed balance, their Ca-ATP cycle gives a K_d of 1.5 nM for profilin-binding nucleotide-free actin, quite different from our measured value of 34 nM with a different profilin and actin.

The equilibrium constants provide important insights about the effect of profilin on the kinetics of nucleotide exchange. Since profilin reduces the affinity of actin for Mg-ATP only 3-fold, while increasing the rate of Mg-ATP dissociation 8-fold, profilin must also *increase* the rate of nucleotide association nearly 3-fold. This is reasonable, because ATP binding is much slower than the diffusion limit (*25*), suggesting that the site is inaccessible. Thus, a conformational change that opens the nucleotide-binding pocket and increases the rate of dissociation is expected to increase the rate of association as well. On the other hand, profilin reduces the affinity of actin for Mg-ADP 24-fold, while increasing the rate of Mg-ADP dissociation 14-fold (Figure 4B), so, in contrast to Mg-ATP, Mg-ADP binds the actin−profilin complex about half as fast as free actin. ADP binds slower than ATP (*53*, *25*), so association may involve a conformational change rather than a simple collision and the binding mechanisms may differ for the two nucleotides.

These effects of profilin on nucleotide affinity and exchange rates presumably arise from alteration of the conformation of the nucleotide-binding pocket. Although the conformation of actin in the crystal of the actin−profilin complex studied by Schutt et al. (*38*) is very similar to the actin subunit in both the actin−DNase complex (*54*) and the actin−gelsolin S1 complex (*55*), the nucleotide-binding pocket is more exposed in new crystal forms of the actin−profilin complex (*56*). These two conformations differ little in energy (*56*) and may be in equilibrium. Profilin may enhance nucleotide dissociation by stabilizing the open conformation. A shift toward an open conformation may also explain why Mg-ATP binds faster to the actin−profilin complex.

Since profilin enhances the rate of Mg-ADP dissociation, but not association, the net result is rapid exchange of any Mg-ADP for Mg-ATP in an ATP-rich environment like the cell. Thus, profilin may contribute to the observed saturation of actin with ATP in cellular extracts (*22*) in those cells with profilins that enhance the rate of nucleotide exchange. Perelroizen et al. (*50*) argued that enhancement of nucleotide

exchange by profilin is not physiologically relevant, based on an absence of an effect of a plant profilin on nucleotide exchange of muscle actin in vitro (*50*) and the ability of plant profilins to substitute for endogenous profilins in yeast (*57*) and *Dictyostelium* (*58*). We suggest having an open mind about this question until assays are available to assess nucleotide exchange in these cells, particularly since profilin can overcome the inhibition of ADP exchange by proteins in the ADF/cofilin family (L. Blanchoin and T. D. Pollard, submitted for publication).

Role of Profilin in Regulating Actin Polymerization in the Cell. Knowledge of the equilibrium constants for profilin-binding actin monomers (*12, 18, 23*; current work) and of the effects of profilin on assembly at the two ends of actin filaments (*9*−*12*) makes it possible to predict the distribution of actin and profilin under cellular conditions. The approach used by Perelroizen et al. (*23*) was to make reasonable assumptions and to use the equilibrium constants to calculate the concentrations of the various species. They assumed that (i) all barbed ends and no pointed ends of actin filaments are capped in resting cells, (ii) the free actin monomer concentration equals the critical concentration at the pointed end (taken to be 0.5 μM), and (iii) a hypothetical cell with a total profilin concentration of 50 μM, total thymosin-β4 concentration of 100 μM, and no other sequestering proteins. Using K_ds of 0.1 μM for profilin and 1.0 μM for thymosin-β4 binding muscle Mg-ATP actin monomers, they calculated equilibrium cellular concentrations of 33 μM for thymosin−actin and 41.5 μM for profilin−actin. It was not clear if these reactions account for the pool of unpolymerized actin in the hypothetical cell, because the total unpolymerized actin was not specified. The assumptions that pointed ends are uncapped and that free actin is 0.5 μM have not been verified and may be false, given the existence of a high-affinity pointed end capping complex in cells (*59*). The assumption that profilin binds muscle and cytoplasmic actin with the same affinity also needs to verified.

We took a different approach to account for the pool of unpolymerized actin—measure the cellular concentrations of the relevant proteins and then use equilibrium constants to calculate if the known proteins can account for the pool of unpolymerized actin. In the case of *Acanthamoeba*, most of the required information is available. *Acanthamoeba* contains approximately 200 μM total actin (*60*), about half of which is polymerized (*2*). Profilin, present at a concentration of 100 μM (*28*), binds ATP-actin monomers with a higher affinity ($K_d = 0.1$ μM) than ADP-actin. Actophorin, present at 20 μM (*61*), binds ADP-actin monomers with higher affinity ($K_d = 0.1$ μM) than ATP-actin (L. Blanchoin and T. D. Pollard, submitted for publication). Profilin and actophorin compete for binding actin monomers (*16*) but have different effects on actin elongation. Profilin−actin elongates barbed ends but not pointed ends so that it can sequester actin if barbed ends are capped. Actophorin−actin elongates both ends, so it does not sequester actin, except to the extent that it prevents profilin binding to ADP-actin (L. Blanchoin and T. D. Pollard, submitted for publication). The proportions of ATP- and ADP-actin monomers in live amoebas are not known, but most of the unpolymerized actin in *Xenopus* extracts is ATP-actin (*22*). Actobindin may also sequester some actin, but its affinity is 10-fold lower than profilin, so its effect on the free actin monomer concentration is much less important than profilin.

Acanthamoeba contains proteins that cap both ends of actin filaments with nanomolar affinity. The Arp2/3 complex [total concentration about 2 μM *(62)*] caps pointed ends (*59*), and capping protein [total about 1 μM (*63*)] caps barbed ends (*64*). The concentrations of both classes of capping proteins appear to exceed the concentration of filament ends in the cell, about 0.2 μM, given 100 μM polymerized actin and filaments of 500 subunits. Therefore, at any point in time, most barbed ends should be capped (*65*). The same argument applies to the pointed end. Occasional interactions with membrane polyphosphoinositides or other uncharacterized regulatory mechanisms may uncap some of the barbed ends and nucleating processes generate new barbed ends (*59*).

Given these concentrations and equilibrium constants and assuming that only profilin sequesters actin monomers, we calculate cellular concentrations of 3 μM free ATP−actin, 97 μM ATP−actin−profilin, and 3 μM free profilin. Any free actin with bound ADP will form a stable complex with actophorin, but the concentration is low, because profilin stimulates the exchange of ADP for ATP (L. Blanchoin and T. D. Pollard, submitted for publication). Biochemical measurements on concentrated cell extracts and immunochemical measurements on extracts and fixed cells all support the conclusion that the majority of the amoeba's profilin is bound to actin (D. A. Kaiser, V. K. Vinson, D. B. Murphy and T. D. Pollard, submitted for publication). A pool of 97 μM Mg-ATP−actin bound to profilin will elongate any uncapped barbed ends at a rate greater than 500 subunits/s, a rate more than sufficient to account for the extension of lamellapodia at the advancing edge of a motile amoeba, about 0.1 μm/s (*66*).

The calculated concentration of 3 μM free actin is higher than the critical concentration for polymerization at either end (0.1 μM at barbed ends and 0.7 μM at pointed ends). If one assumes that the free actin concentration must be less than or equal to one or both of these critical concentrations, additional sequestering proteins are required. However, the cellular concentrations of actin and profilin should be reevaluated, since small adjustments of the published values might account for the unpolymerized actin pool without resorting to other sequestering proteins. On the other hand the free actin concentration might actually be higher than either critical concentration, since both ends may be capped most of the time and since spontaneous nucleation is unfavorable.

REFERENCES

1. Bray, D., and Thomas, C. (1976) *J. Mol. Biol. 105*, 527−544.
2. Gorden, C., Boyer, J. L., and Korn, E. D. (1977) *J. Biol. Chem. 252*, 8300−8309.
3. Blikstad, I., Markey, F., Carlsson, L., Persson, T., and Lindberg, U. (1978) *Cell 15*, 935−943.
4. Pollard, T. D. (1986) *J. Cell Biol. 103*, 2747−2754.
5. Machesky, L. M., and Pollard, T. D. (1993) *Trends Cell Biol. 3*, 381−385.
6. Mockrin, S. C., and Korn, E. D. (1980) *Biochemistry 19*, 5359−5362.
7. Nishida, E. (1985) *Biochemistry 24*, 1160−1164.
8. Goldschmidt-Claremont, P. J., Machesky, L. M., Doberstein, S. K., and Pollard, T. D. (1991) *J. Cell Biol. 113*, 1081−1089.
9. Pollard, T. D., and Cooper, J. A. (1984) *Biochemistry 23*, 6631−6641.

10. Kaiser, D. P., Sato, M. D., Ebert, R., and Pollard, T. D. (1986) *J. Cell Biol. 102*, 221−226.
11. Pring, M., Weber, A., and Bubb, M. R. (1992) *Biochemistry 31*, 1827−1836.
12. Pantaloni, D., and Carlier, M.-F. (1993) *Cell 75*, 1007−1014.
13. Bubb, M., Lewis, M. S., and Korn, E. D. (1991) *J. Biol. Chem. 266*, 3820−3826.
14. Nachmias, V. T. (1993) *Curr. Opin. Cell Biol. 5*, 56−62.
15. Moon, A., and Drubin, D. (1995) *Mol. Biol. Cell 6*, 1423−1431.
16. Maciver, S. K., Zot, H. G., and Pollard, T. D. (1991) *J. Cell Biol. 115*, 1611−1620.
17. Carlier, M.-F., Laurent, V., Santolini, J., Melki, R., Didry, D., Xia, G. X., Hong, Y., Chua, N. H., and Pantaloni, D. (1997) *J. Cell Biol. 136*, 1307−1322.
18. Perelroizen, I., Marchand, J., Blanchoin, L., Didry, D., and Carlier, M.-F. (1994) *Biochemistry 33*, 8462−8478.
19. Machesky, L. M., Atkinson, S. J., Ampe, C., Vandekerckhove, J., and Pollard, T. D. (1994) *J. Cell Biol. 127*, 107−115.
20. Reinhard M., Giehl, K., Abel, K., Haffner, C., Jarchau, T., Hoppe, V., Jockusch, B. M., and Walter, U. (1995) *EMBO J. 14*, 1583−1589.
21. Mullins, R. D., Kelleher, J. F., Xu, J., and Pollard, T. D. (1998) *Mol. Biol. Cell 9*, 841−852.
22. Rosenblatt, J., Peluso, P., and Mitchison, T. J. (1995) *Mol. Biol. Cell. 6*, 227−236.
23. Perelroizen, I., Carlier, M.-F., and Pantaloni, D. (1995) *J. Biol. Chem. 270*, 1501−1508.
24. Kasai, M., Nakano, E., and Oosawa, F. (1965) *Biochim. Biophys. Acta 94*, 494−503.
25. De La Cruz, E. M., and Pollard, T. D. (1995) *Biochemistry 34*, 5452−5461.
26. Ho, S. N., Hunt, H. D., Horton, R. M., Pullen, J. K., and Pease, L. R. (1989) *Gene 77*, 51−59.
27. Kaiser, D. A., Goldschmidt-Clermont, P. J., Levine, B., and Pollard, T. D. (1989) *Cell Motil. Cytoskel. 14*, 251−262.
28. Tseng, P. C.-H., Runge, M. S., Cooper, J. A., Williams, J. C., Jr., and Pollard, T. D. (1984) *J. Cell Biol. 98*, 214−221.
29. Deakin, H. Ord, M. G., and Stoken, L. A. (1963) *Biochem. J. 89*, 296−304.
30. Pollard, T. D. (1984) *J. Cell Biol. 99*, 769−777.
31. Spudich, J. A., and Watt, S.(1971) *J. Biol. Chem. 246*, 4866−4871.
32. Houk, T. W., and Ue, K. (1974) *Anal. Biochem. 62*, 66−74.
33. Cooper, J. A., Walker, S. B., and Pollard, T. D. (1983) *J. Muscle Res. Cell Motil. 4*, 253−262.
34. Ampe, C., Sato, M., Pollard, T. D., and Vandekerckhove, J. (1988) *Eur. J. Biochem. 170*, 597−601.
35. Petrella, E. C., Machesky, L. M., Kaiser, D. A., and Pollard, T. D. (1996) *Biochemistry 35*, 16535−16543.
36. Machesky, L. M., Goldschmidt-Clermont, P. J., and Pollard, T. D. (1990) *Cell Regul. 1*, 937−950.
37. Fedorov, A. A., Magnus, K. A., Graupe, H., Lattman, E. E., Pollard, T. D., and Almo, S. C. (1994) *Proc. Natl. Acad. Sci. U.S.A. 91*, 8636−8640.
38. Schutt, C. E., Myslik, J. C., Rozychi, M. D., Goonesekere, N. C., and Lindberg, U. (1993) *Nature 365*, 810−816.
39. Archer, S. J., Vinson, V. K., Pollard, T. D., and Torchia, D. A. (1994) *FEBS Lett. 337*, 145−151.
40. Jameson, D. M., and Sawyer, W. H. (1995) *Methods Enzymol. 246*, 283−300, Academic Press, NY.
41. Tobacman, L., and Korn, E. D. (1982) *J. Biol. Chem. 257*, 4166−4170.
42. Tseng, P. C.-H., and Pollard, T. D. (1982) *J. Cell Biol. 94*, 213-218.
43. Malm, B. (1984) *FEBS Lett. 173*, 399−402.
44. Goldschmidt-Claremont, P. J., Furman, M. I., Wachsstock, D., Safer, D., Nachmias, V. T., and Pollard, T. D. (1992) *Mol. Biol. Cell 3*, 1015−1024.
45. Safer, D., Sosnick, T. R., and Elzinga, M. (1997) *Biochemistry 36*, 5806−5816.
46. Carlier, M.-F., Jean, C., Rieger, K. J., Lenfant, M., and Pantaloni, D. (1993) *Proc. Nat. Acad. Sci. U.S.A. 90*, 5034−5038.
47. Tarachandani, A., and Wang, Y. (l996) *Cell Motil. Cytoskel. 34*, 313−323.
48. Lee, S., Li, M., and Pollard, T. D. (1988) *Anal. Biochem. 168*, 148−155.
49. Lal, A. A., and Korn, E. D. (1985) *J. Biol. Chem. 260*, 10132−10138.
50. Perelroizen, I., Didry, D., Christensen, H., Chua, N., and Carlier, M.-F. (1996) *J. Biol. Chem. 271*, 12302−12309.
51. Pollard, T. D., Goldberg, I., and Schwarz, W. H. (1992) *J. Biol. Chem. 267*, 20339−20345.
52. Kinosian, H. J., Selden, L. A., Estes, J. E., and Gershman, L. C. (1993) *J. Biol. Chem. 268*, 8683.
53. Nowak, E., and Goody, R. S. (1988) *Biochemistry 27*, 8613−8617.
54. Kabsch, W., Mannherz, H., Such, D., Pai, E., and Holmes, K. (1990) *Nature 347*, 37−44.
55. McLaughlin, P. J., Gooch, J. T., Mannherz, H.-G., and Weeds, A. G. (1993) *Nature 364*, 685−692.
56. Chik, J. K., Lindberg, U., and Schutt, C. E. (1996) *J. Mol. Biol. 263*, 607−623.
57. Christensen, H. E. M., Ramachandran, S., Tan, C.-T., Surana, U., Dong, C.-H., and Chua, N.-H. (1996) *Plant J. 10*, 263−279.
58. Karakesisoglou, I., Schleicher, M., Gibbon, B. C., and Staiger, C. J. (1996) *Cell Motil. Cytoskel. 34*, 36−47.
59. Mullins, R. G., Heuser, J., and Pollard, T. D. (1998) *Proc. Natl. Acad. Sci. U.S.A. 95*, 6181−6186.
60. Pollard, T. D., and Korn, E. D. (1973) *Cold Spring Harbor Symp. Quantum Biol. 37*, 573−583.
61. Cooper, J. A., Blum, J. D., Williams, R. C., Jr., and Pollard, T. D. (1986) *J. Biol. Chem. 261*, 477−485.
62. Kelleher, J. F., Atkinson, S. J., and Pollard, T. D. (1995) *J. Cell Biol. 131*, 385−397.
63. Cooper, J. A., Blum, J. D., and Pollard, T. D. (1984) *J. Cell Biol. 99*, 217−225.
64. Isenberg, G. H., Aebi, U., and Pollard, T. D. (1980) *Nature 288*, 455−459.
65. Schafer, D. A., Jennings, P. B., and Cooper, J. A. (1996) *J. Cell Biol. 135*, 169−179.
66. Sinard, J. H., and Pollard, T. D. (1989) *Cell Motil. Cytoskel. 12*, 42−52.

BI980093L